# Water Treatment by Dielectric Barrier Discharge Tube with Vapor Flow

T. Shibata[1] and H. Nishiyama[2]
[1]Formly Graduate School of Engineering, Tohoku University, Japan
[2]Institute of Fluid Science, Tohoku University, Japan

**Abstract—Non-thermal plasma technologies with water vapor have been developed for a wide range of applications. In this study, a water treatment which introduces a vaporized solution into a coaxial dielectric barrier discharge (DBD) tube using Ar was investigated experimentally. To clarify the organic decomposition characteristics, acetic acid was decomposed by this treatment. A diluted acetic acid solution was vaporized by a water vaporizer in advance and introduced into the DBD tube. The residence time of the water vapor introduced into the discharge area in a DBD tube was approximately 6–8 ms. Acetic acid was effectively decomposed and the decomposition ratio reached almost 70% for small water flow rate, despite the short residence time, which is superior to the mist plasma treatment.**

**Keywords—Water treatment, DBD tube, vapor flow, organic pollutants**

## I. Introduction

The use of non-thermal plasma is an effective method to decompose pollutants because of its ability to produce reactive species, such as ozone and free radicals, with low input power [1]. Recently, non-thermal plasma has been paid attention, not only for gas purification but also for water purification. A useful feature of the plasma treatment is its ability to suppress pollution. Organic compounds can be decomposed completely by plasma to produce water and carbon dioxide ($CO_2$). Ozone treatment is a well-known water treatment method utilizing non-thermal plasma [2]. Ozone generated by non-thermal plasma in the gas phase is transported into the processing liquid. However, in this treatment, a part of the ozone and almost all of the free radicals are decomposed by themselves and disappeared during transportation. Because of the short life times of these reactive species, plasma must be generated near the processing solution to utilize them more effectively. Therefore, various discharge methods that employ direct contact with water (e.g., direct discharge in water [3], above water [4], in bubbles [5], and introducing water spray into a discharge [6]) have been studied for the utilization of these free radicals for water treatment.

Plasmas with water vapor were developed for a wide range of applications such as hydrogen isotope exchange [7], [8], fossil fuel (methane biogas and gasoline) reforming [9]–[13], hydrogen generation from water or alcohols [14]–[16], and sterilization [17]. Some toxic pollutants cannot be decomposed by conventional chemical and biological treatment methods. To decompose persistent organics, it is necessary to utilize OH with higher oxidation potential in spite of its short life time. The dielectric barrier discharge (DBD) with mist flow method of water treatment investigated in our previous study [18] can utilize these radicals; however, an OH radical dissolution process is still required. Furthermore, the high energy electrons in a non-thermal plasma are unable to react directly with dissolved wastes. If the wastes also exist in a gas phase, the high energy electrons can react with waste directly in the case of vapor flow treatment. Therefore, there is potential to improve the water treatment efficiency by discharging the water as a vaporized phase since the plasma can be directly generated in the waste-water vapor. It should be noted that much energy is necessary to vaporize water; however, for industrial water treatment, the thermal energy of waste heat from energy systems can be effectively utilized for the vaporization of water.

In this study, a water treatment method which involves vaporizing a solution and introducing it into a coaxial DBD tube with Ar carrier gas was investigated experimentally. The discharge power and light emission were analyzed as the discharge characteristics of the DBD tube. The hydrogen peroxide generation, electrical conductivity, and solution pH variations were measured as liquid properties. Acetic acid decomposition was also demonstrated in order to evaluate the decomposition characteristics of the persistent organics. In order to investigate the water vapor effect, the supply water flow rate was important operating parameter which was controlled by the liquid source vaporization system. Finally, the decomposition efficiency and system energy efficiency as a function of the decomposition ratio using water vapor flow was compared with that of mist plasma treatment, where the treated solution was atomized by the ultrasonic device before introduction into a coaxial DBD tube [18].

## II. Experimental setup and procedure

Fig. 1 shows the schematic illustration of the experimental setup, which consists of a water vaporizer, DBD tube, and cooling tube. The DBD tube was made of alumina with 2 mm thickness and 6 mm inner diameter. The inner grounded electrode was a tungsten rod with 3 mm diameter which was supported by silicon plugs and located along the central

Corresponding author: Hideya Nishiyama
e-mail address: nishiyama@ifs.tohoku.ac.jp

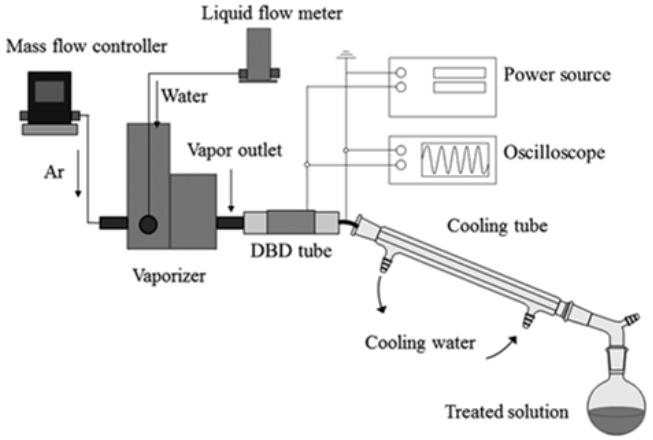


Fig. 1. Schematic illustration of experimental setup.

axis of the tube [18]. The length of the grounded electrode, which approximately equals the length of the plasma region, was 50 mm. The gap between the inner wall of the tube and the central electrode was, therefore, 1.5 mm. A copper tape powered electrode encased the outer tube to avoid an electrical short circuit with liquid vaporizer. A high voltage power amplifier (TREK, INC., MODEL 10/40A-HS) was used to apply a sinusoidal ac voltage to the DBD tube. The voltage amplitude was $\pm 10$ kV (20 $kV_{pp}$) and the voltage frequency was 1,000 Hz. Ar was supplied as the carrier gas at a flow rate ($Q_{\mathrm{Ar}}$) of 5 l/min by a mass flow controller (MC-20SLPM-D/5M, Alicat) and the water flow rate ($Q_w$) was controlled from 0.1 g/min to 2.0 g/min. Purified water or an acetic acid solution was used as the processing solution for the measurement of liquid property or organic compounds decomposition characteristics, respectively. Supplied water and carrier gas were vaporized and heated to 170°C by a liquid source vaporization system (MV-2000, HORIBA), which controls the water flow rate and vaporization. Combined with the liquid mass flow meter (SEF-E40), water can be supplied at a stable flow rate by feedback control.

The voltage was measured by an electric voltage probe (Tektronix, P6015A). The electric charge was determined by measuring the voltage applied to an inserted capacitor (0.1 $\mu$F).

The introduced water vapor flow passed through the DBD tube only once. After passing through the DBD tube, the water vapor was condensed by the cooling tube, in which iced water was used as a coolant. The temperature of the iced water was set at approximately 283K.

The integrated images of the discharge at various water vapor concentrations were recorded by using a Nikon digital camera. The exposure time was 1/30 s, the ISO speed was 1600, and the F-number was 5.6.

The dissolved $H_2O_2$ concentration as a final product was measured by a coulometric titrator (Hiranuma Sangyo, HP-300) to evaluate the chemical reactivity. The $H_2O_2$ concentration of the collected solution was measured after leaving several hours, in order to terminate finish the chemical reaction in the treated liquid because other oxidants may give the influence on the $H_2O_2$ measurement. $H_2O_2$ is one of the well-known indicator of OH radical generation as shown following reactions;

$$\begin{aligned} \mathrm{OH + OH} &\longrightarrow \mathrm{H_2O_2} \\ \mathrm{HO_2 + HO_2} &\longrightarrow \mathrm{H_2O_2 + O_2} \\ \mathrm{OH + HO_3} &\longrightarrow \mathrm{H_2O_2 + O_2} \end{aligned}$$

The solution pH and electrical conductivity were measured by the glass electrode and AC-2-electrode methods, respectively. The initial electrical conductivity and pH of acetic acid solution were approximately 80 $\mu$S/cm and 5.5, respectively. The initial acetic acid concentration was approximately 105 mg/l. It was diluted 10,000 times by purified water. Hydrogen generation was measured by gas chromatography (GC). GC measurements were performed with a barrier discharge ionization detector (SHIMADZU, BID-2010 Plus). Acetic acid decomposition and generation of by-products, such as formic acid were measured by using ion chromatography to evaluate the characteristics of persistent organic pollutants (POPs) decomposition. Ion chromatography measurements were conducted with an electrical conductivity detector using a Shim-pack IC-A3 column with a solution of 4-hydroxybenzonic acid (6.37 mM), bis-tris (2.55 mM), and boric acid (39.9 mM), and a flow rate of 1.2 ml/min. The solution was sampled before vaporization (initial solution) and after treatment (condensed solution).

## III. Results and discussion

### A. Discharge characteristics of DBD tube with vapor flow

Fig. 2 shows the time integrated images of discharge of vapor flow at various water flow rates and DBD mist flow for tentative comparison. The discharge emission intensity decreases visibly with the water flow rate. The time averaged discharges are relatively uniform in the circumferential direction across an annular gap for vapor flow. On the other hand, there is the non-uniform discharge showing large regions without discharge in the DBD tube for DBD mist flow, which results from the electric field concentration by condensed water film on the electrode or alumina tube as previously reported [18]. This means that the water vapor is diffused uniformly in the DBD tube until the flow rate of 1.5 g/min. Exceptionally, there is a small region in which discharge cannot be occurred because of the water vapor condensation, which occurs only when the water flow rate is 2.0 g/min.

Figs. 3(a) and (b) show the Q-V Lissajous figure and discharge power ($P_d$), respectively, calculated using the Q-V Lissajous figure. The Q-V Lissajous figures are expanded for the applied voltage axis by increasing the supplied water flow rate. The discharge power increases from 3 to 6 W and becomes saturated with the increase in water flow rate because more power is needed to discharge the water vapor compared with dry Ar due to required dissociation energy prior to ionization. In this study, the highest input power ($\sim$6 W) is obtained with a water flow rate greater than 1.5 g/min.

### B. Liquid properties

Fig. 4 shows the dissolved $H_2O_2$ concentration ($C_{\mathrm{H_2O_2}}$ (mg/l)) and energy yield for $H_2O_2$ generation

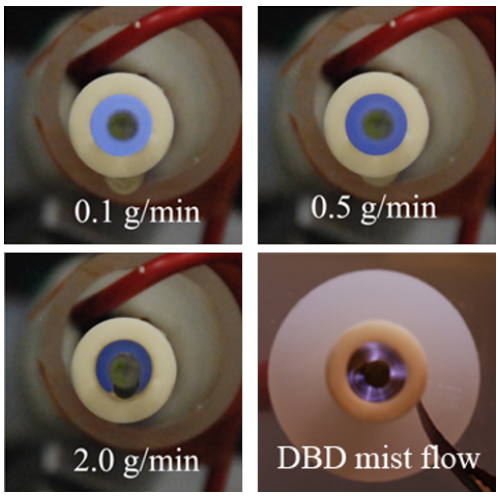


Fig. 2. Photos of discharge with various water flow rates.

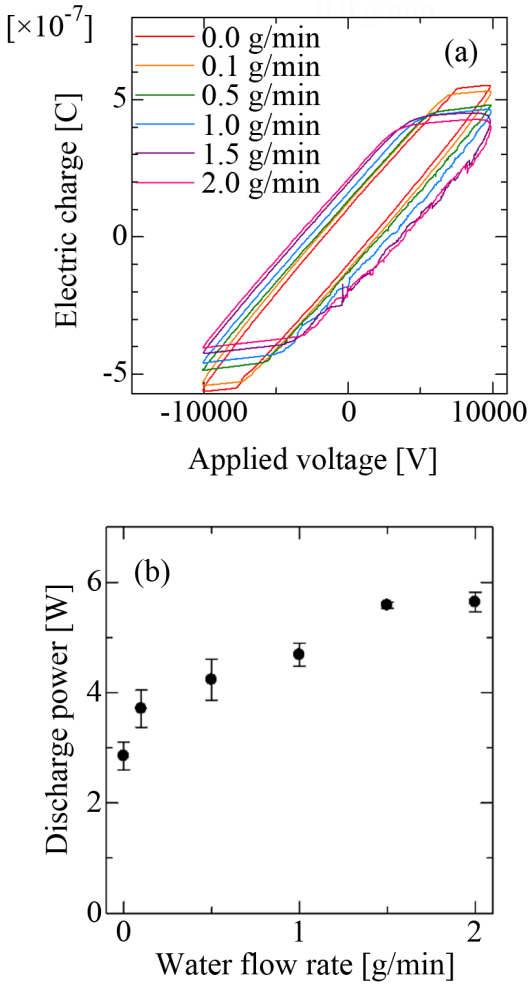


Fig. 3. Q-V Lissajous figure (a) and calculated discharge power (b) with various water flow rates. Error bars shows the standard deviation.

($\omega_{H_2O_2}$ (mol/J)) for pure water. The energy yield for $H_2O_2$ generation is calculated as follows:

$$\omega_{H_2O_2} = \frac{C_{H_2O_2}/(34.01 \times 1000)V_l}{P_d t} \quad (1)$$

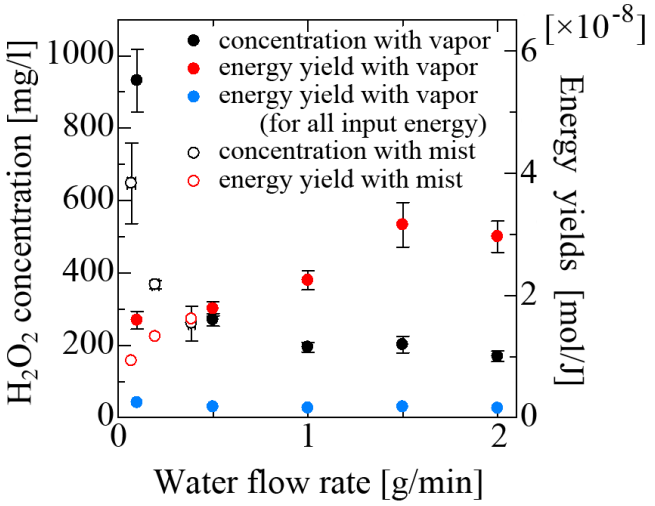


Fig. 4. $H_2O_2$ generation characteristics with various water flow rates. (Filled circles and open circles show the results with the vapor and mist flow respectively. Black, Red and blue results show the $H_2O_2$ concentrations, energy yields only for discharge energy and energy yields for all energy including energies for discharge and vaporizing together. Purified water is used as a source of vapor and mist. The discharge power is varied from 3 to 6 W with frequency of 1000 Hz.) Error bars shows the standard deviation.

where $V_l$ is solution volume ($l$) collected in the processing time $t$ (s), $P_d$: discharge power (W).

The discharge power is 3–6 W. The initial electrical conductivity and solution pH of purified water are about 0.0 $\mu$S/cm and 7.0, respectively to measure the liquid properties including experimental uncertainty.

The main reaction for $H_2O_2$ generation is recombination of the OH generated by the water dissociation reaction because this system includes only $H_2O$ and Ar. A high $H_2O_2$ concentration is obtained with a low water flow rate and decreases exponentially with an increase in the water flow rate because the specific input energy decreases. The specific input energy $\eta$ (J/g) is defined as the ratio of discharge power $P_d$ (W) to water flow rate $Q_w$ (g/min) as follows;

$$\eta = \frac{P_d}{Q_w} \times 60 \quad (2)$$

In this study, the highest $H_2O_2$ concentration (~900 mg/l) is obtained with a water flow rate of 0.1 g/min. The energy yield for $H_2O_2$ generation increases with an increase in the water flow rate. However, the energy yield is (mol/J) saturated for $3.2 \times 10^8$ above a water flow rate of 1.5 g/min. If the vaporization energy is considered, the system energy yield for all input energy drops to 0.082–0.25 ($\times 10^8$ mol/J) as shown by blue full circle in Fig. 4 for comparison. The $H_2O_2$ concentration and energy yield obtained by the mist treatment are also shown in Fig. 4. These two water treatment methods show almost the same concentration and energy yield for $H_2O_2$ generation with the low water flow rate. However, the water treatment method with water vapor flow can be operated throughout a wider range of water flow rates. Therefore, a higher energy yield is obtained by the water vapor treatment for larger water flow rates.

Figs. 5 and 6 show the electrical conductivity and solution pH after plasma treatment, respectively. The initial electrical

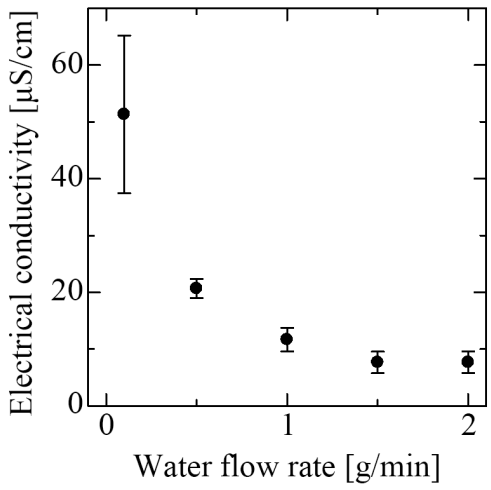


Fig. 5. Electrical conductivity of treated solution with various water flow rates (discharge power 3–6 W, frequency 1000 Hz, initial electrical conductivity 80 $\mu$S/cm). Error bars shows the standard deviation.

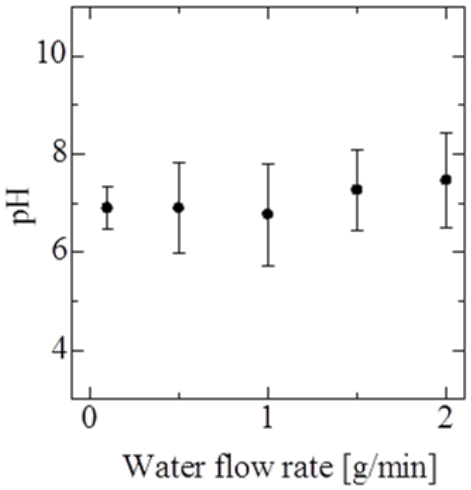


Fig. 6. Solution pH of treated solution with various water flow rates (discharge power 3-6 W, frequency 1000 Hz, initial pH 7–8). Error bars shows the standard deviation.

conductivity and solution pH are approximately 0 $\mu$S/cm and 7, respectively. The electrical conductivity increases with the plasma treatment because dissolved $H_2O_2$ is weakly ionized. Therefore, the electrical conductivity decreases with the water flow rate because the $H_2O_2$ concentration decreases with an increase in the water flow rate. In contrast, the solution pH is almost unchanged by the discharge because nitrogen oxides (NOx) cannot be generated in this system. Although concentrations of $NO_3^-$, which is the main acid generated by NOx in such a plasma system, are also measured, the $NO_3^-$ concentration level is below the measurement limit.

### *C. Acetic acid decomposition*

To evaluate the characteristics of persistent organic decomposition, acetic acid was used as the target of decomposition. Although acetic acid and water are not azeotropes, the liquid source vaporization system can completely vaporize the

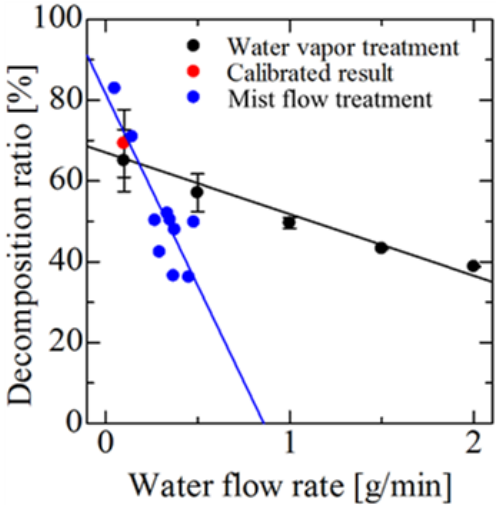


Fig. 7. Acetic acid decomposition ratio with various water flow rates. (Decomposition ratio of mist flow treatment is also shown for comparison. Red filled circle shows the calibrated result and solid line shows the fitting line.) Error bars shows the standard deviation.

mixture. In addition, the temperature of the liquid source vaporization system was set to 443K and acetic acid is thermally decomposed above 453K [19]. Therefore, the acetic acid concentration is not changed by vaporization energy.

Fig. 7 shows the acetic acid decomposition ratio ($\gamma$) at various water flow rates. The acetic acid concentration is calibrated only at a water flow rate of 0.1 g/min because the acetic acid concentration is changed only by vaporization. The acetic acid decomposition ratio is calculated by using following equation:

$$\gamma = \left(1 - \frac{C_{Ac}}{C_0}\right) \times 100 \tag{3}$$

where, $C_{Ac}$ (mg/l) is the acetic acid concentration in the condensed solution after treatment and $C_0$ (mg/l) is the initial acetic acid concentration. The decomposition ratio decreases almost linearly with an increase in the water flow rate because the specific input energy decreases with increase in the water flow rate. The highest decomposition ratio in this study is approximately 70% at a water flow rate of 0.1 g/min. The decomposition ratio with the mist flow treatment is also shown in Fig. 7 for comparison. Within the range of low water flow rates, the mist flow treatment shows higher decomposition ratio. However, at water flow rates greater than 0.3 g/min, the water vapor treatment shows a higher decomposition ratio compared with that of the mist flow treatment. The condensed water film is difficult to be formed on the DBD inner electrode for water vapor treatment compared with the mist treatment. Therefore, the DBD can be easily generated and kept stably in the case of water vapor treatment without forming water film due to the condensation. In addition, the operational range of the treated water flow rate is 4 times wider more than that of the mist treatment. Therefore, a larger amount of solution can be treated by the water vapor treatment compared with mist flow, although the decomposition ratio decrease to 40% at 2 g/min.

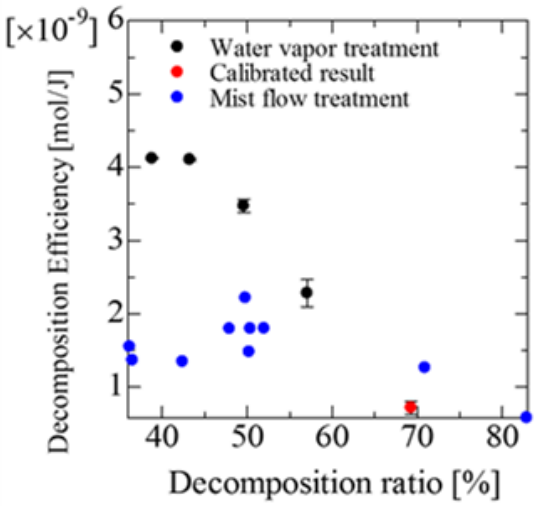


Fig. 8. Acetic acid decomposition efficiency with decomposition ratio. (Efficiency of mist flow treatment is also shown for comparison. Red filled circle shows the calibrated result.) Error bars shows the standard deviation.

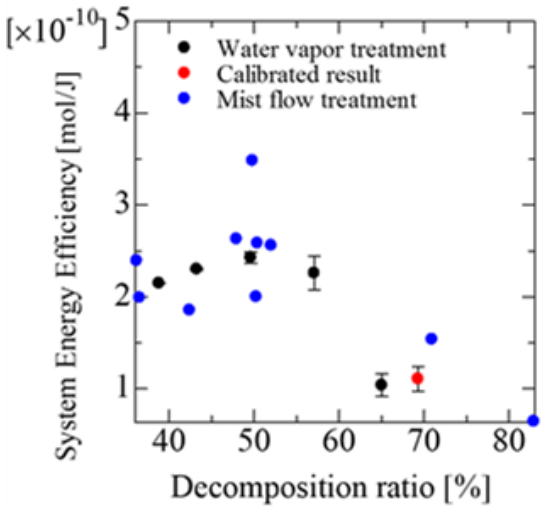


Fig. 9. System energy efficiency for acetic acid decomposition with decomposition ratio. (Efficiency of mist flow treatment is also shown for comparison. Red filled circle shows the calibrated result.) Error bars shows the standard deviation.

Fig. 8 shows the acetic acid decomposition efficiency ($\omega_{Ac}$ (mol/J)) as a function of acetic acid decomposition ratio defined by Eq. (3) for the same flow rate. The acetic acid decomposition efficiency is defined by the following equation:

$$\omega_{Ac} = \frac{C_0/(60.05 \times 1000)V_l}{P_d t} \times \frac{\gamma}{100} \tag{4}$$

The decomposition efficiency using the mist flow treatment is also shown in Fig. 8. The water vapor treatment shows higher energy efficiency for lower decomposition ratio (which means high treatment amount) compared with mist flow treatment. The decomposition efficiency increases up to $\sim 4 \times 10^9$ mol/J but the decomposition ratio is saturated at almost 40% in the present system. Furthermore, comparison with the decomposition efficiency for acetic acid with other different systems was made. The previous energy efficiency for discharged bubble jet system is $0.648 \times 10^9$–$2.08 \times 10^9$ (mol/J) [5].

Fig. 9 shows the system energy efficiency for acetic acid decomposition, considering the energies of vaporization and atomization. Both treatment methods show almost same system energy efficiency and trends for decomposition ratio. This is because the water vapor treatment requires much energy for vaporizing a larger amount of treatment liquid compared with the ultrasonic atomization. However, the energy cost of the water vapor treatment can be reduced by utilizing the waste heat from industrial thermal systems without using electrical energy to increase the system energy efficiency.

## IV. Conclusions

A novel water treatment method using water vapor flow in a DBD tube was developed. The obtained results are summarized as follows.

1) A time-averaged uniform light emission is observed from the dielectric barrier discharge in water vapor-Ar mixture gases. A few power DBD can be stably generated in a vapor flow without forming condensation water film instead of that in a mist flow.
2) Higher concentrated $H_2O_2$ is obtained by the DBD with vapor flow than with mist flow. The highest $H_2O_2$ concentration is obtained with a low water flow rate. On the other hand, the highest energy yield is obtained with a high water flow rate.
3) The electrical conductivity increases with using DBD, especially with a lower water flow rate in which the highly concentrated $H_2O_2$ is weakly ionized in water. The solution pH is almost the same around 7 because nitric acid cannot be generated in this study.
4) The highest decomposition ratio of acetic acid in vapor flow system is approximately 70% at a water vapor flow rate of 0.1 g/min. The decomposition efficiency of vapor flow is significantly larger than that of mist flow treatment until decomposition ratio of 60%. The highest efficiency ($4 \times 10^9$ mol/J) is obtained at a water flow rate of 1.5 g/min, which is larger than that of discharged bubble jet.
5) The higher acetic acid decomposition efficiency is achieved compared with those of the mist flow treatment because a larger amount of water can be treated by vapor flow treatment. When the vapor is generated by the waste heat from the thermal systems energy instead of electrical heating, the system energy efficiency can be increased significantly.

## Acknowledgment

This work was partly supported by a Grant-in-Aid for JSPS Fellows (249008). The authors are thankful to Associate

Professor Hidemasa Takana and Dr. Satoshi Uehara for their valuable discussions and further Mr. Tomoki Nakajima for his technical support with IFS, Tohoku University, Japan.

## REFERENCES

[1] V. I. Parvulescu, M. Magureanu, and P. Lukes, Eds., *Plasma Chemistry and Catalysis in Gases and Liquids*. Wiley-VCH Verlag GmbH & Co. KGaA, 2012.

[2] T. Shibata, A. Ozaki, H. Takana, and H. Nishiyama, "Water treatment characteristics using activated air microbubble jet with photochemical reaction," *Journal of Fluid Science and Technology*, vol. 6, pp. 242–251, 2011.

[3] A. A. Joshi, B. R. Locke, P. Arce, and W. C. Finney, "Formation of hydroxyl radicals, hydrogen peroxide and aqueous electrons by pulsed streamer corona discharge in aqueous solution," *Journal of Hazardous Materials*, vol. 41, pp. 3–30, 1995.

[4] N. Takeuchi, R. Oishi, Y. Kitagawa, and K. Yasuoka, "Adsorption and efficient decomposition of perfluoro compounds at plasma-water interface," *IEEE Transactions on Plasma Science*, vol. 39, pp. 3358–3363, 2011.

[5] H. Nishiyama, K. Niinuma, S. Shinoki, and H. Takana, "Decomposition of acetic acid using multiple bubble jets with pulsed electrical discharge," *Plasma Chemistry and Plasma Processing*, vol. 35, pp. 339–354, 2015.

[6] R. Burlica, K.-Y. Shih, and B. R. Locke, "Formation of $H_2$ and $H_2O_2$ in a water-spray gliding arc nonthermal plasma reactor," *Industrial and Engineering Chemistry Research*, vol. 49, pp. 6342–6349, 2010.

[7] H. J. Kim, Y. D. Park, and W. M. Lee, "Hydrogen isotope exchange reactions in an electrical discharge," *Plasma Chemistry and Plasma Processing*, vol. 20, pp. 259–275, 2000.

[8] I. G. Koo and W. M. Lee, "Hydrogen isotope exchange reactions in an atmospheric pressure discharge utilizing water as carrier gas," *Plasma Chemistry and Plasma Processing*, vol. 24, pp. 537–554, 2004.

[9] T. Paulmier and L. Fulcheri, "Use of non-thermal plasma for hydrocarbon reforming," *Chemical Engineering Journal*, vol. 106, pp. 59–71, 2005.

[10] M. G. Sobacchi, A. V. Saveliev, A. A. Fridman, L. A. Kennedy, S. Ahmed, and T. Krause, "Experimental assessment of a combined plasma/catalytic system for hydrogen production via partial oxidation of hydrocarbon fuels," *International Journal of Hydrogen Energy*, vol. 27, pp. 635–642, 2002.

[11] H. Kabashima and S. Futamura, "Continuous production of synthesis gas at ambient temperature from steam reforming of methane with nonthermal plasma," *Chemistry Letters*, pp. 1108–1109, 2002.

[12] Y.-F. Wang, C.-H. Tsai, W.-Y. Chang, and Y.-M. Kuo, "Methane steam reforming for producing hydrogen in an atmospheric-pressure microwave plasma reactor," *International Journal of Hydrogen Energy*, vol. 35, pp. 135–140, 2010.

[13] J. L. Hueso, V. J. Rico, J. Cotrino, J. M. Jiménez-Mateos, and A. R. González-Elipe, "Water plasmas for the revalorisation of heavy oils and cokes from petroleum refining," *Environmental Science and Technology*, vol. 43, pp. 2557–2562, 2009.

[14] R. Burlica, K.-Y. Shih, B. Hnatiuc, and B. R. Locke, "Hydrogen generation by pulsed gliding arc discharge plasma with sprays of alcohol solutions," *Industrial and Engineering Chemistry Research*, vol. 50, pp. 9466–9470, 2011.

[15] H. Kabashima, H. Einaga, and S. Futamura, "Hydrogen generation from water, methane, and methanol with nonthermal plasma," *IEEE Transactions on Industry Applications*, vol. 39, pp. 340–345, 2003.

[16] I. G. Koo, M. Y. Choi, J. H. Kim, J. H. Cho, and W. M. Lee, "Microdischarge in porous ceramics with atmospheric pressure high temperature $H_2O/SO_2$ gas mixture and its application for hydrogen production," *Japanese Journal of Applied Physics*, vol. 47, pp. 4705–4709, 2008.

[17] T. Furui and T. Sato, "Sterilization efficacy of steam plasma flow at atmospheric pressure," *Transactions of the Japan Society of Mechanical Engineers, Part B*, vol. 74, pp. 879–883, 2008.

[18] T. Shibata and H. Nishiyama, "Acetic acid decomposition in a coaxial dielectric barrier discharge tube with mist flow," *Plasma Chemistry and Plasma Processing*, vol. 34, pp. 1331–1343, 2014.

[19] Y. Matsui, N. Takeuchi, K. Sasaki, R. Hayashi, and K. Yasuoka, "Experimental and theoretical study of acetic-acid decomposition by a pulsed dielectric-barrier plasma in a gas-liquid two-phase flow," *Plasma Sources Science and Technology*, vol. 20, 2011.